Deletions in Epidermal Keratins Leading to Alterations in Filament Organization In Vivo and in Intermediate Filament Assembly In Vitro

Pierre A. Coulombe, Yiu-mo Chan, Kathryn Albers, and Elaine Fuchs

Howard Hughes Medical Institute, Departments of Molecular Genetics and Cell Biology and of Biochemistry and Molecular Biology, The University of Chicago, Chicago, Illinois 60637

Abstract. To investigate the sequences important for assembly of keratins into 10-nm filaments, we used a combined approach of (*a*) transfection of mutant keratin cDNAs into epithelial cells in vivo, and (*b*) in vitro assembly of mutant and wild-type keratins. Keratin K14 mutants missing the nonhelical carboxy- and amino-terminal domains not only integrated without perturbation into endogenous keratin filament networks in vivo, but they also formed 10-nm filaments with K5 in vitro. Surprisingly, keratin mutants missing the highly conserved L L E G E sequence, common to all intermediate filament proteins and found at the carboxy end of the α-helical rod domain, also assembled into filaments with only a somewhat reduced efficiency. Even a carboxy K14 mutant missing ~10% of the rod assembled into filaments, although in this case filaments aggregated significantly. Despite the ability of these mutants to form filaments in vitro, they often perturbed keratin filament organization in vivo. In contrast, small truncations in the amino-terminal end of the rod domain more severely disrupted the filament assembly process in vitro as well as in vivo, and in particular restricted elongation. For both carboxy and amino rod deletions, the more extensive the deletion, the more severe the phenotype. Surprisingly, while elongation could be almost quantitatively blocked with large mutations, tetramer formation and higher ordered lateral interactions still occurred. Collectively, our in vitro data (*a*) provide a molecular basis for the dominance of our mutants in vivo, (*b*) offer new insights as to why different mutants may generate different phenotypes in vivo, and (*c*) delineate the limit sequences necessary for K14 to both incorporate properly into a preexisting keratin filament network in vivo and assemble efficiently into 10-nm keratin filaments in vitro.

INTERMEDIATE filaments (IFs)[1] are composed of proteins (40–210 kD) with a remarkable capacity to self-assemble into complex 10 nm filaments (for reviews, see Weber and Geisler, 1987; Aebi et al., 1988). All IF proteins form coiled-coil dimers, a unique feature imparted by the nature of their sequences (Parry et al., 1977; Ahmadi and Speakman, 1978; McLachlan, 1978; Quinlan and Franke, 1982; Woods and Inglis, 1984; Quinlan et al., 1984). The typifying feature of IF polypeptides is a central, 310 amino acid α-helical rod domain (360 for lamins) with heptad repeats of hydrophobic residues (McLachlan, 1978; Geisler and Weber, 1982; Hanukoglu and Fuchs, 1982; McKeon et al., 1986; Fisher et al., 1986). Dimers are aligned in parallel and in register (Parry et al., 1977; Aebi et al., 1986), and are further stabilized by periodic ionic interactions (Parry et al., 1977; McLachlan and Stewart, 1982; Henderson et al., 1982).

In contrast to other IF proteins, which can form homodimers and assemble into homopolymers, keratins form heterodimers (Coulombe and Fuchs, 1990; Hatzfeld and Weber, 1990; Steinert, 1990). While type I and type II keratins are often expressed as specific pairs in vivo (for review, see Sun et al., 1984), almost any combination of the two types in vitro will result in 10-nm filaments (Franke et al., 1983; Hatzfeld and Franke, 1985). Despite the similarity in structure among all keratin filaments, filament properties and intracellular interactions vary substantially. For instance, epidermal keratin subunits and IFs seem to be more stable than those of simple epithelial cells (Steinert et al., 1976; Franke et al., 1983; Coulombe and Fuchs, 1990; Steinert, 1990).

The mechanisms leading to higher ordered packing of all IF dimers are complex. Tetramers form readily both in vivo and in vitro, and scanning transmission electron microscopy has revealed that ~32 polypeptides, or 8 tetramers, contribute to the overall width of the filament (Steven et al., 1983; Engel et al., 1985). Each 10-nm filament is subdivided into four intertwined protofibrils, suggesting that two tetramers compose the lateral diameter of a protofibril (see Aebi et al.,

K. Albers' present address is Department of Pathology, University of Kentucky, Lexington, KY 40536–0093.

1. *Abbreviation used in this paper*: IF, intermediate filament.

1988). Although the arrangement of tetramers in the protofibril is unknown, an IF of 40 μm in length would be expected to be composed of protofibrils containing 500–800 hypothetical octameric units linked in an end-to-end fashion. For many IF proteins, the entire 10-nm assembly process can take place in vitro, in the absence of auxiliary proteins.

Since all IF proteins share some sequence similarities and generate 10-nm filaments with similar structure, it has been assumed that sequences required for filament formation will be similar. Suggestive evidence has been provided by IF cDNA deletion mutagenesis and transfection studies showing that deletion of highly conserved residues at the ends of the α-helical rod caused both alterations in cytoskeletal 10-nm filament networks (Albers and Fuchs, 1987, 1989; Van den Heuvel et al., 1987; Gill et al., 1990; Wong and Cleveland, 1990; Raats et al., 1990; Lu and Lane, 1990) and disruptions in nuclear lamina assembly (Loewinger and McKeon, 1988; Heald and McKeon, 1990). In the absence of electron microscopic data or in vitro filament assembly studies, however, it could not be ascertained whether the resulting IF mutant proteins truly caused alterations in IF assembly, or alternatively, alterations in IF networks resulting from perturbations in either IF stability or associated protein–IF interactions.

The roles of the more variable nonhelical end domains in IF assembly and organization are even less clear than those of the α-helical rod segment. Early in vivo and in vitro studies of filament formation suggested that the carboxy tail sequences of some IF proteins might be dispensable in the IF assembly process (Bader et al., 1986; Kaufmann et al., 1985; Albers and Fuchs, 1987; van den Heuvel et al., 1987; Lu and Lane, 1990). Other studies have revealed possible roles for the carboxy tails in IF network assembly (Gill et al., 1990; Wong and Cleveland, 1990; Lu and Lane, 1990), IF–nuclear interactions (Georgatos and Blobel, 1987*a*, *b*), and nuclear lamina disassembly during mitosis (Loewinger and McKeon, 1988; Heald and McKeon, 1990). Studies have also suggested that at least for some IF proteins, the amino-terminal domains may have a number of important functions as well (Sauk et al., 1984; Kaufmann et al., 1985; Georgatos et al., 1985; Georgatos and Blobel, 1987*a*; Gill et al., 1990; Wong and Cleveland, 1990; Raats et al., 1990; Lu and Lane, 1990; Heald and McKeon, 1990). That nonhelical end domains are important for some IF networks is underscored by the fact that these domains of type III and type V IFs contain specific phosphorylation sites that appear to play a role in the mitosis-mediated reorganization or disassembly of these IFs in some cell types (Inagaki et al., 1987; Evans, 1988, 1989; Geisler and Weber, 1988; Geisler et al., 1989; Kitamura et al., 1989; Chou et al., 1989; Heald and McKeon, 1990; Peter et al., 1990; Ward and Kirschner, 1990). The end domains are also phosphorylation sites for other IFs that do not show cell cycle–mediated changes, although the functional significance of phosphorylation in these cases is not yet known (see for example Steinert, 1988). Thus, while end domains of many IFs seem to be important for the dynamics of filament assembly in vivo and for cytoarchitecture of IF networks, the role of end domains in 10-nm filament formation per se is not clear, nor is it known whether they have functions common to all IF proteins.

It seems likely that assembly of each IF network will be governed by some molecular principles unique to each 10-nm cyto or nuclear skeleton. Clearly, even for a single IF, a multifaceted approach is required to sort out which IF sequences are involved in filament assembly, filament stability, and establishment of intermediate filament cytoskeletons. Several years ago, using deletion mutagenesis and mammalian gene transfer, we began to analyze sequences important for epidermal keratin filament network formation in vivo (Albers and Fuchs, 1987, 1989). We have now constructed bacterial clones that overexpress each of the carboxy-terminal and amino-terminal mutants that we studied in vivo. We have purified human K14 mutant polypeptides and examin their ability in vitro to form tetramers and filaments wit wild-type human K5, in the absence or presence of wild-type K14. We have compared our in vitro analyses with the effects of these mutants on filament organization in human simple epithelial and stratified squamous epithelial cells in culture. Our in vitro data have enabled us (*a*) to determine the behavior of mutant type I keratins in tetramer formation and filament assembly; (*b*) to assess the importance of wild-type K14 in the assembly of mutant K14s into IFs; and (*c*) to develop new insights into our understanding of the various mutant phenotypes that we have observed in our in vivo studies.

Materials and Methods

Construction of Plasmid pJK14P and Deletion Mutants for Mammalian Gene Transfection Studies

(a) pJK14P. The construction of plasmid pJK14P has been described previously (Albers and Fuchs, 1987). The parent vector, pJay1, is a mammalian expression vector, containing a polylinker cloning region 3′ from the SV-40 early promoter and enhancer. The insert (K14P) contains the complete 5′ noncoding and coding portion of the cDNA encoded by the gene for the human K14 (Hanukoglu and Fuchs, 1982; Marchuk et al., 1984), with the exception that the sequences encoding the last five carboxy amino acids of the K14 protein have been replaced by a sequence coding for the last five carboxy-terminal residues of the neuropeptide substance P (see Fig. 1). Following the TGA stop codon is the 3′ noncoding sequence of a *Drosophila* hsp70 gene (Albers and Fuchs, 1987). The insert was cloned in the 5′ to 3′ direction into the Hind III/Sma I sites of plasmid pJay1.

(b) COOH-terminal and NH_2-terminal Deletion Mutants. Details of the constructions of the carboxy terminal deletion mutants are given in Albers and Fuchs (1987). Mutants were designated as pJK14PCΔX, where X denotes the number of encoded K14 carboxy-terminal amino acid residues missing from the pJK14P construct. For example, pJK14PCΔ42 corresponds to a mutant which encodes the P-tag two residues past the highly conserved L L E G E sequence at the end of the α-helical rod domain. Details of the constructions of the NH_2-terminal mutants are given in Albers and Fuchs (1989). Mutants were designated as pJK14PNΔX, where X is the number of encoded amino acid residues missing from the amino-terminal end of human K14. For example, pJK14P NΔ107 corresponds to a K14 mutant that begins at two amino acid residues before the start of the α-helical rod domain.

Construction of pETK14, pETK14P, pETK5 and pETK14P Deletion Mutants for Overexpression in Escherichia coli

Construction of plasmids pETK14 and pETK5 was described previously (Coulombe and Fuchs, 1990). As a consequence of the cloning procedure, sequences encoding the first two amino acids (Thr-Thr) of human K14 were changed to sequences encoding a single Ala residue. Plasmid pETK14P was made by replacing the fragment from pETK14 with the corresponding fragment from pJK14P. The K14P deletions mutants were transferred from their pJay1 mammalian expression vectors to the bacterial expression plasmid pETK14P by standard subcloning procedures. The carboxy-terminal deletions were transferred either as Kpn I-Avr II fragments or Kpn I-Bam HI

(partial) fragments (Fig. 1). The amino-terminal deletions NΔ107 and NΔ131 were transferred as Nco I-Kpn I fragments. To generate pETK14PNΔ115, pETK14P was digested with Nco I and Bste II, treated with Klenow to fill in the 5′ sticky ends, and treated with T4 DNA ligase to allow self-ligation. To generate K14PNΔ150, pETK14P was digested with Nco I, treated with Klenow, digested with Kpn I, treated with mung bean exonuclease, and finally treated with T4 DNA ligase to allow self-ligation. The double deletion mutant K14PNΔ107CΔ42 was made by subcloning the K14PNΔ107 fragment into pETK14PCΔ42 as described above. The junctions of all constructs were verified using DNA sequence analysis.

DNA Transfections and Immunofluorescent Labeling

Cells were transfected with mutant cDNAs as described by Albers and Fuchs (1987). At 65-h posttransfection, cells were fixed in methanol. To detect K14 substance P-tagged proteins, we used a rabbit anti-P polyclonal antiserum from Wako Chemicals (Dallas, TX). The mouse monoclonal antibody LE-41 (Lane, 1982) was used to identify the endogenous PtK2 keratin network. A rabbit polyclonal anti-K5 peptide antisera was used to identify the endogenous SCC-13 keratin network (Lersch, R., and E. Fuchs, unpublished data). To visualize the primary antibody, we used FITC-conjugated goat anti-rabbit IgG (Cappel) and either Texas Red-conjugated goat anti-rabbit IgG (Cappel Laboratories, Malvern, PA) or Texas red-conjugated goat anti-mouse IgG (Tago Inc., Burlingame, CA).

Overexpression of Keratins in E. coli and FPLC Purification

Bacterial clones of BL21(DE3), transformed with plasmids pETK5, pETK-14, pETK14P, or any of the pETK14PCΔX or pETK14PNΔX mutants, were cultured and induced to express keratins as described previously (Coulombe and Fuchs, 1990). The specificity of keratin expression was evaluated by SDS PAGE and immunoblot analyses of total protein extracts of the transformed BL21(DE3) cells.

Purification of keratins from total bacterial proteins was achieved by isolation of inclusion bodies and either one or two rounds of FPLC™ anion exchange chromatography (Mono Q; Pharmacia Inc., Piscataway, NJ) in 6 M urea buffer as described previously (Coulombe and Fuchs, 1990). Final peak fractions were then pooled and stored at −70°C until needed. Before use, samples were concentrated and desalted by ultrafiltration through Centricon-10 units, as specified by the manufacturer (Amicon, W. R. Grace and Co., Boston, MA). This purification scheme resulted in keratin fractions of >95% purity, as determined by gel scanning densitometry.

Keratin Complex Formation/Isolation, In Vitro Reconstitution of Filaments, and Gel Filtration Chromatography

Pure preparations of K5 and K14P or K14PΔX mutants in 6 M urea-Tris buffer were obtained by ion exchange chromatography, and the protein concentrations were measured by the Bradford assay (Bradford, 1976). K5 and K14P samples were then mixed in the desired ratio (usually a slight molar excess of K5 unless specified otherwise) in a final volume of 1–1.25 ml and at a final concentration of 1 mg/ml. After a few minutes at room temperature, K5-K14P mixtures were then stored at 4°C until further processed. K5-K14P complexes formed in 6 M urea buffer were separated from uncomplexed K5 or K14P using anion-exchange chromatography (Mono Q) as described above. Fractions were collected and analyzed by SDS-PAGE and Coomassie blue staining.

For in vitro filament assembly, two different procedures were used. In the first one, pure preparations of K5 and K14P (or K14P mutants) were mixed in ~1:1 molar ratio at a concentration of 200–300 μg/ml and equilibrated by dialysis against a 9 M urea buffer containing 10 mM Tris·HCl, 10 mM β-mercaptoethanol, 0.3 mg/ml PMSF, pH 7.2, at room temperature. Additional dialyses were then performed against 5 mM Tris·HCl, 10 mM β-mercaptoethanol, pH 7.2, for 2 h at room temperature, followed by 10 h at 4°C, and finally 10 mM Tris·HCl, 10 mM β-mercaptoethanol, pH 7.2 for 2 h at 4°C. Alternatively, a K5-K14P (or mutant K14) complex was first isolated by anion exchange chromatography in 6 M urea. The complex (150–250 μg/ml) was then dialyzed against a buffer consisting of 6 M urea, 10 mM Tris·HCl, 10 mM β-mercaptoethanol, 0.3 mg/ml PMSF, pH 7.2, for 2 h at room temperature, followed by dialysis against non-urea, low Tris buffers as in the first method. This alternative method had the advantage of providing a K5-K14P mixture in a perfect 1:1 molar ratio as starting material. When K14P deletion mutants were assayed for 10-nm filament formation in vitro, a control sample containing K5-K14P at the same protein concentration was always run in parallel. The reconstituted samples were then stored at 4°C until examination under a Philips CM10 electron microscope.

For tetramer analysis, K5-K14P complexes isolated by anion exchange chromatography were subjected to gel filtration chromatography in the presence of molecular mass standards as described by Coulombe and Fuchs (1990).

Electron Microscopy of Keratin Filaments and Quantitative Measurements

Carbon-coated nickel grids were glow discharged before applying the specimen. Keratin filament samples were diluted ~1:3–1:5 with 10 mM Tris-HCl, pH 7.2, and a 5-μl aliquot was adsorbed on a pretreated grid for 30 s. Grids were then washed gently with several drops of 10 mM Tris·HCl buffer (1 min) and H_2O, and negatively stained for 30 s with 1.25% uranyl acetate. Excess stain was removed by blotting with filter paper. Specimens were examined in a Philips CM-10 electron microscope operated at an acceleration voltage of 80 kV. Magnification was calibrated using a diffraction grating replica (No. 10021; Ernest Fulham, Inc. NY).

For quantitation of filament width and length, random series of eight micrographs from each experimental condition tested were printed at a final magnification of either 100,000 or 140,000X. Lengths were measured from 40 randomly selected filaments. Widths were measured from 16 randomly selected filaments. Quantitative analyses were made using the MacMeasure software program on an Apple microcomputer.

Results

Constructing Plasmids of Mutant and Wild-type Keratins for Expression in Mammalian Cells and in Bacteria

Previously, we subcloned full-length and truncated cDNAs encoding normal and mutant forms of the human epidermal keratin K14 into the mammalian expression vector pJay1 (Albers and Fuchs, 1987). This vector contained an SV-40 promoter and enhancer to drive expression of these keratins in a variety of mammalian cell types. To follow expression of wild type and mutant forms of K14 in both epidermal ($K14^+$, $K5^+$) and simple epithelial ($K8^+$, $K18^+$) cells, we placed a tag encoding the antigenic portion of neuropeptide substance P just 5′ from the TGA stop codon of the K14 cDNA sequences. This tag did not interfere with the ability of K14 to integrate into a keratin filament network (Albers and Fuchs, 1987) or to form filaments in vitro (Coulombe and Fuchs, 1990). The P-tagged full-length construct is referred to as pJK14P (Fig. 1).

To produce large quantities of human K5 and K14 for filament assembly studies, we subcloned full-length cDNAs encoding a substance P-tagged human K14 and its partner K5 into the bacterial expression plasmid pET-8c (Coulombe and Fuchs, 1990). The resultant keratin cDNA plasmids are called pETK14P and pETK5, respectively (Fig. 1). To conduct in vitro studies on the keratin mutants that we had already examined by gene transfection, we also introduced the mutant K14 cDNAs into the pET-8c plasmid. Fig. 1 illustrates the mutant keratin cDNAs that were introduced into mammalian and bacterial expression plasmids for the present studies. N*ΔX* and C*ΔX* refer to NH_2-terminal and COOH-terminal deletions, respectively, with *X* being the number of amino acid residues removed from the K14P sequence as a consequence of the deletion. The rod is shown subdivided into four segments (Fig. 1, *1A*, *1B*, *2A*, and *2B*) according to the position of predicted perturbations in the α-helix (Hanukoglu and Fuchs, 1982). For direct compari-

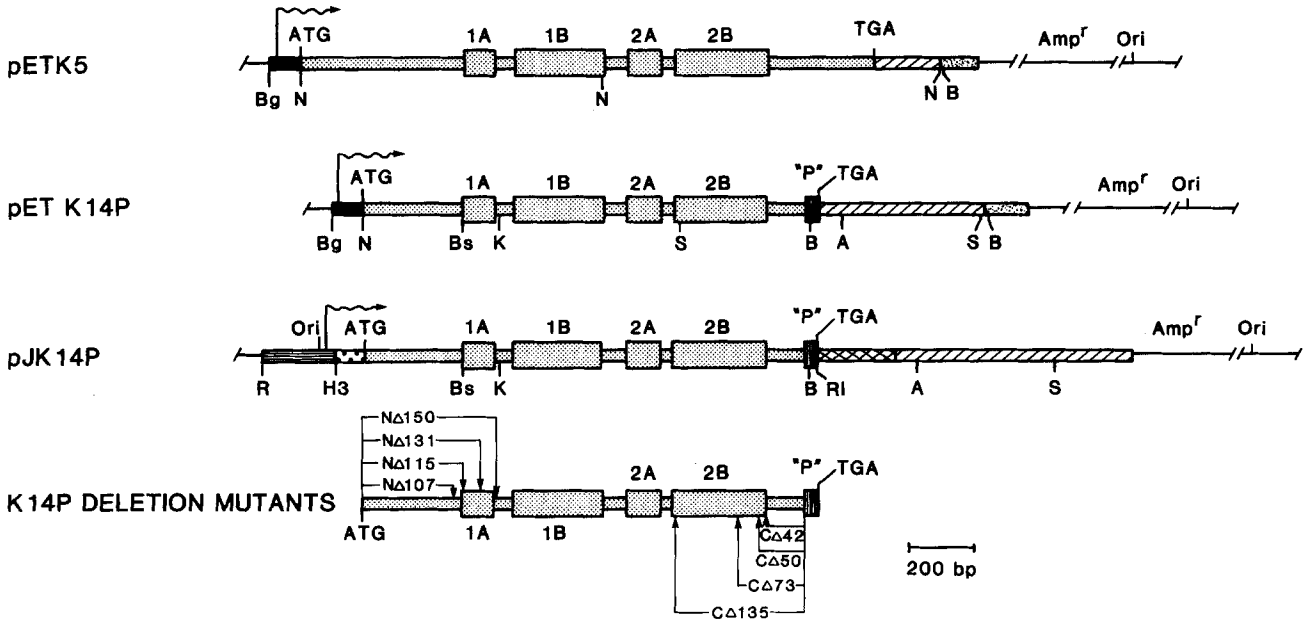

Figure 1. Genetic map of plasmids pETK5, pETK14P, pJK14P, and K14 mutants. Details of plasmid constructions can be found in Materials and Methods. Components are represented as follows. Promoters: black box, T7 RNA polymerase promoter; horizontal lined boxes, SV-40 major early promoter; squiggly arrow, transcription initiation site. For pET constructs, 5′-untranslated sequence is part of the vector. For pJay1 constructs, 5′-untranslated sequence is from human K5 or K14 cDNAs. Coding sequences: boxes with small dots, complete coding segments of human K5 and K14 cDNAs. K14P constructs miss sequences encoding the five carboxy-terminal amino acid residues, and have been replaced by sequences encoding the carboxy-terminal domain of neuropeptide substance P (vertical lined box marked "P"). Large boxes designated 1A, 1B, 2A, and 2B represent α-helical domains as predicted by secondary structure methods (Hanukoglu and Fuchs, 1982). Coding sequences of deletion mutations for both pET and pJay1 constructs are indicated on the bottom construct, and are referred to as NΔX, where *X* designates the number of amino acid residues missing from the NH_2 terminus of K14P; or CΔX, where *X* designates the number of amino acid residues missing from the COOH terminus of K14P. 3′ Sequences: diagonal-lined boxes in pET constructs, 3′ noncoding sequences to either human K5 or human K14 genes; box with ×'s, 3′ noncoding sequences and polyadenylation signal of the *Drosophila* hsp70 gene (Albers and Fuchs, 1987); 3′ stippled boxes, transcription terminator sequences in pET-8c; 3′ diagonal-lined boxes in pJay1 constructs, a mixture of *Drosophila* and vector sequences from pAHP.2 (see Albers and Fuchs, 1987). Plasmid sequences: *Ori*, origin of replication; *amp*, ampicillin resistance gene. Restriction endonuclease sites are: *Bg*, Bgl I; *N*, Nco I; *S*, Sac I; *Bs*, Bste II; *K*, Kpn I; *B*, Bam HI; *A*, Avr II; *R*, Eco RI; *H3*, Hind III.

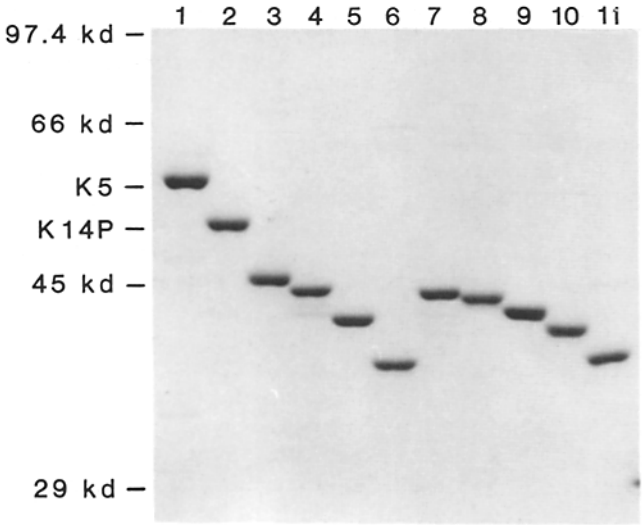

Figure 2. SDS-PAGE analyses of keratin purification. Purified keratin mutants were analyzed by electrophoresis through 8.5% polyacrylamide SDS gels and visualized by staining with Coomassie blue. Lane *1*, K5; lane *2*, K14P; lane *3*, K14PCΔ42; lane *4*, K14PCΔ50; lane *5*, K14CΔ73; lane *6*, K14PCΔ135; lane *7*, K14PNΔ107; lane *8*, K14PNΔ115; lane *9*, K14PNΔ131; lane *10*, K14PNΔ150; lane *11*, K14PNΔ107/CΔ42. Molecular masses of protein standards are indicated at left in kilodaltons.

sons with in vivo studies, the P-tag was retained for all of our in vitro constructs.

Mutant and wild-type keratins were isolated from solubilized inclusion body fractions and purified by ion exchange chromatography in 6 M urea buffer (Coulombe and Fuchs, 1990). Fig. 2 illustrates the purity of the wild-type K5, K14P, and mutant K14P used for these studies.

The Nonhelical Ends of K14P Are Not Required for Filament Assembly In Vitro

When equimolar amounts of wild-type K5 and K14P in 6–9 M urea buffer were dialyzed against a low salt buffer at neutral pH (see Materials and Methods), extensive 10-nm filaments were formed as judged by electron microscopic analysis of the dialyzed mixture (Fig. 3 *A*). This was true even when we reduced the keratin concentration to ~35 μg/ml, i.e., the approximate critical concentration necessary for IF

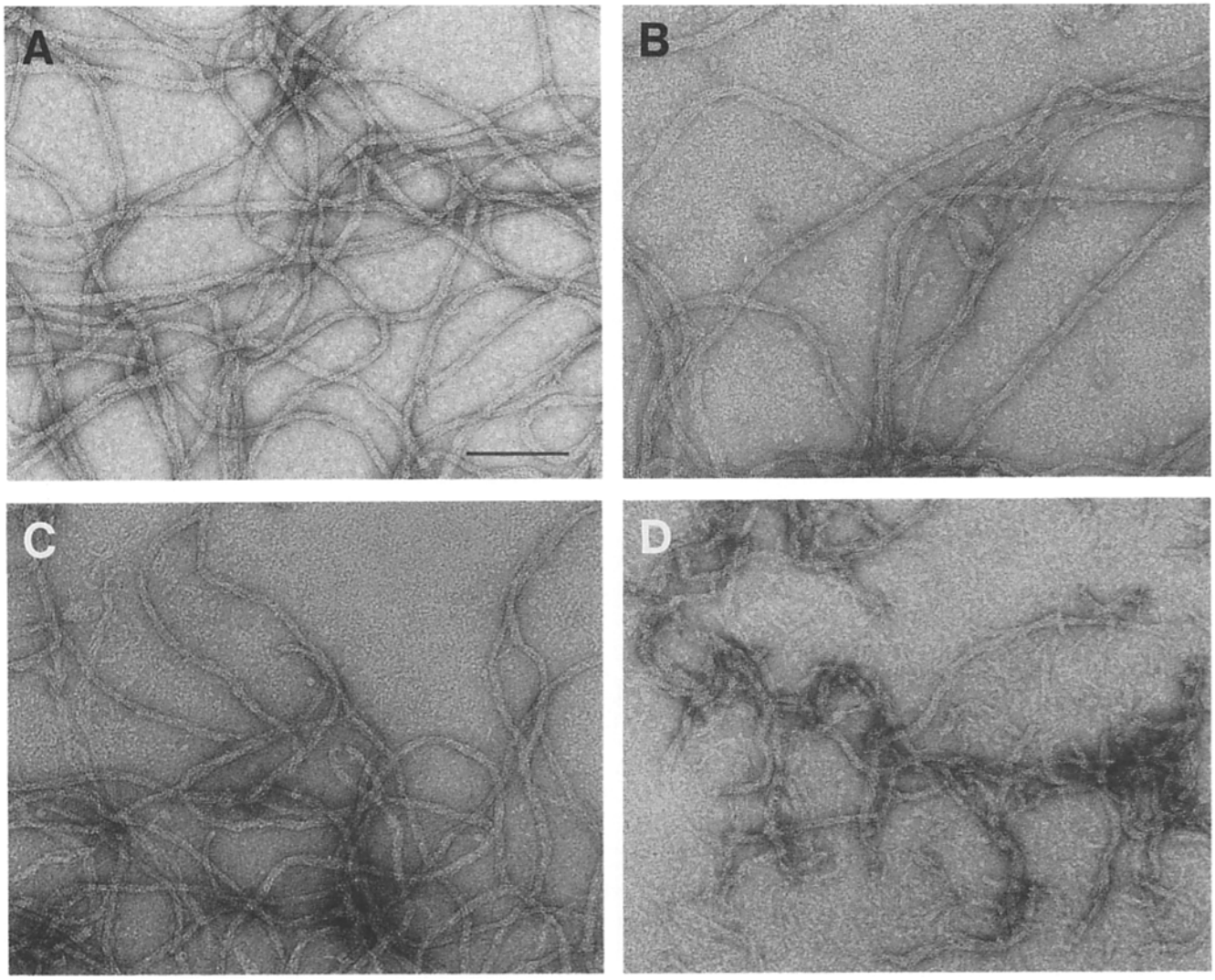

Figure 3. In vitro assembly of purified keratins into filaments. Approximately equimolar amounts of type I and type II keratins from peak fractions of the anion exchange column were combined at a concentration of 250 μg/ml in 9 M urea buffer, and dialyzed twice against non-urea buffers as described in Materials and Methods. Assembled filaments were negatively stained and visualized by electron microscopy. Type I keratins used in combination with wild-type K5 were: *A*, K14P (control); *B*, K14PCΔ42; *C*, K14PNΔ107; *D*, K14PNΔ115. Small amounts of unpolymerized material seen in *B* and *C* are aggregates of the molar excess of one of the two keratin types involved, and could be removed by centrifugation (not shown). Bar, 0.1 μm.

assembly (Steinert et al., 1976). These data were indistinguishable from those obtained with untagged K14 (Coulombe and Fuchs, 1990), indicating that neither the P-tag nor bacterial expression of keratins interfered with the assembly process.

When we combined K5 with K14PCΔ42, missing the entire K14 nonhelical carboxy-terminal domain, 10-nm filaments were formed which were indistinguishable from those assembled from wild-type K14 and K5 (Fig. 3 *B*). This finding was consistent with and extended our in vivo studies on K14PCΔ42, showing that this tailless keratin could integrate into the preexisting network of epidermal keratinocytes ($K14^+$, $K5^+$) or simple epithelial cells ($K8^+$, $K18^+$), without change in phenotype (Albers and Fuchs, 1987).

Previously, we discovered that a headless K14, K14PNΔ107, incorporated without effect into the endogenous keratin network of epidermal and simple epithelial cells in culture (Albers and Fuchs, 1989). Since in vitro and in vivo assembly studies on desmin had shown that a portion of the NH_2 terminus is required for homopolymer formation, but not for heteropolymer formation with wild-type desmin or vimentin (Kaufmann et al., 1985; Raats et al., 1990), we anticipated that K14PNΔ107 might be able to assemble with K5 in vitro to form obligate heteropolymers. On the other hand, recent in vivo studies on NF-L and NF-M have shown that even when present at <10% of the wild-type protein, mutants missing certain internal segments of the nonhelical NH_2-terminal domains disrupted endogenous type III or type IV-containing IF networks (Gill et al., 1990; Wong and Cleveland, 1990). To determine whether our K14PNΔ107 mutant could assemble with K5 in the absence of wild-type type I keratins, we performed in vitro reconstitution studies (Fig.

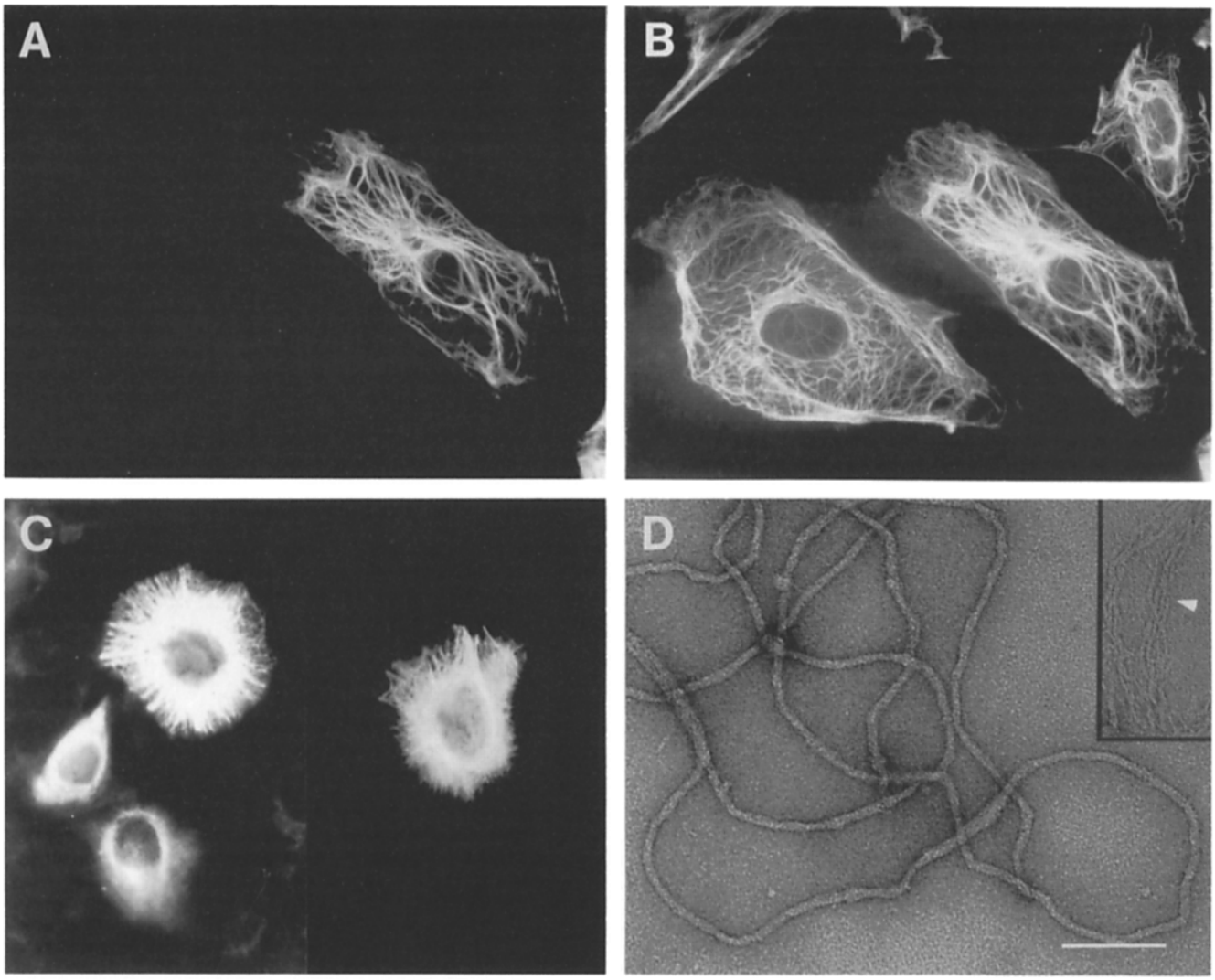

Figure 4. In vivo and in vitro analysis of the headless and tailless K14 mutant, K14PNΔ107/CΔ42. (*A* and *B*) PtK2 simple epithelial cells were transfected with the headless and tailless pJK14PNΔ107/CΔ42. (*C*) SCC-13 keratinocytes were transfected with pJK14P (left side) or pJK14PNΔ107/CΔ42 (right side). The fate of the transfected gene product was examined by double-label immunofluorescence with anti-P (*A* and *C*) and either anti-K8 (LE41) (*B*) or anti-K5 (not shown). Note: in all cases, the foreign gene product integrated into and colocalized with both endogenous keratin networks. (*D*) Purified K5 and K14PNΔ 107/CΔ42 were combined in 6 M urea buffer, and the keratin complex was isolated by anion-exchange chromatography. Peak fractions were pooled and processed for in vitro assembly as described in Materials and Methods. Filaments were negatively stained and visualized by electron microscopy. Note that filaments are only ~8 nm, but the examination of partially unraveled filaments (*inset*) indicates that they are still composed of four protofibrils (*arrowhead*). Bar, 0.1 μm (*D* only).

3 *C*). Our results clearly demonstrate that K14PNΔ107 can assemble in vitro with K5, and furthermore suggest that the differences between the tail mutants of K14, NF-L, and NF-M in vivo cannot be explained simply on the basis of variations in relative amounts of mutant to wild-type IF proteins in the corresponding transfected cells.

Secondary structure predictions have designated the start of α-helical domain 1A as the residue immediately following a highly conserved E-K/R sequence (Hanukoglu and Fuchs, 1982; Geisler and Weber, 1982). However, closer inspection suggests that the seven preceding residues, i.e., L L V G S E K, also have some capacity for α-helix formation (Chou and Fasman, 1978). Since K14PNΔ107 terminated at the boundary of the extended helix, we created a new mutant, K14PNΔ115, which terminated at the boundary of the previously predicted helix. Interestingly, K14PNΔ115 assembled with K5 into filaments in vitro, but they were shorter than normal, and fewer filaments were obtained with this mutant than with the K14PNΔ107 mutant (Fig. 3 *D*, compare with *C*). These data indicate that sequences within the seven aa that distinguish K14PNΔ107 from K14PNΔ115 are important for efficient assembly and for bona fide 10-nm filament structure. It is interesting to note that the four residues preceding the highly conserved E-K/R sequence (L V G S for K14) show some homology among most IF proteins, but the homology then drops precipitously towards the amino termi-

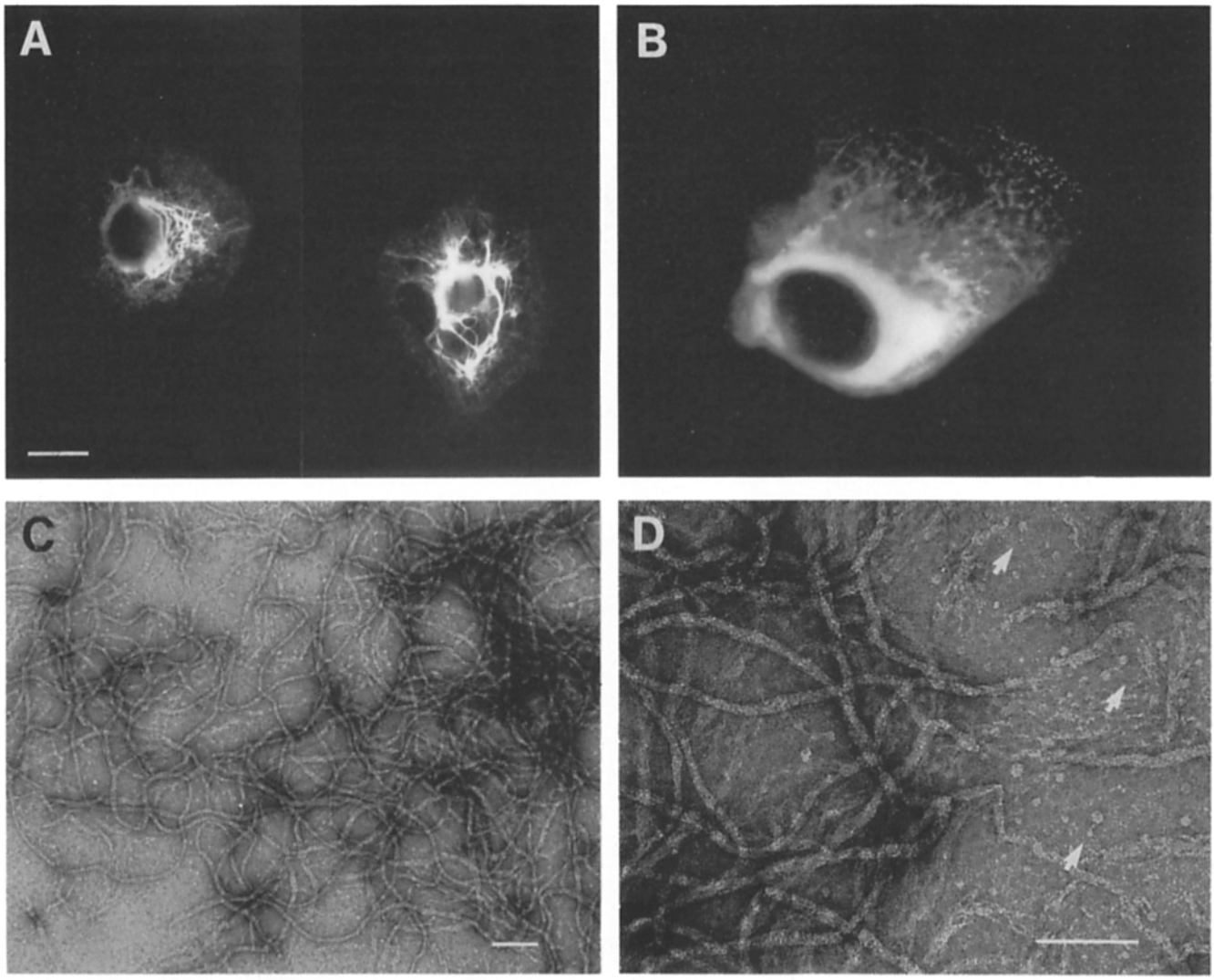

Figure 5. In vivo and in vitro analysis of the L L E G E K14 mutant, K14PCΔ50. (*A* and *B*) PtK2 (*A*) or SCC-13 keratinocytes (*B*) were transfected with the L L E G E deletion derivative pJK14PCΔ50 and processed as described in Materials and Methods. K14PCΔ50 integrated into and colocalized with both endogenous keratin networks, causing a collapse of the filament network. Note that the example shown in *B* was rare: SCC-13 cells transfected with K14PCΔ50 typically gave a wild-type phenotype. (*C* and *D*) K5 and K14PCΔ50 complexes were isolated by chromatography and processed for in vitro assembly and electron microscopy as described in the legend to Fig. 4. Arrows denote unpolymerized material present after assembly. Bars: (*A*) 10 μm; (*C* and *D*) 0.1 μm.

nus. While amino acid sequence homologies, secondary structure predictions and in vitro assembly studies together are not sufficient to unequivocally define the amino boundary of the IF rod, our results suggest that it may be slightly larger than previously anticipated.

When the headless and tailless K14 mutant, K14PNΔ107/CΔ42, was introduced into PtK2 simple epithelial cells in vitro, it integrated without apparent consequence into the preexisting network (Fig. 4 *A*, anti-P; and *B*, anti-K8, respectively; see also Albers and Fuchs, 1989). K14PNΔ107/CΔ42 also integrated without disruption into SCC-13 keratinocytes, and the resulting phenotype was indistinguishable from that of K14PNΔ107, K14PCΔ42, and K14P transfected keratinocytes (see examples in Fig. 4 *C*). From these data, we predicted that the rod domain was able to assemble into functional tetramers, at least in the presence of wild-type type I and type II keratins. We extended these earlier studies to demonstrate that even in complete absence of wild-type K14, K14PNΔ107/CΔ42 assembled into keratin filaments (Fig. 4 *D*). While quantitative studies demonstrated that the diameter of the K5·K14PNΔ107CΔ42 filaments was only ~8 nm, we could still see from occasional unraveled filaments that they were comprised of four protofibrils, and hence were bona fide keratin filaments (Fig. 4 *D*, see *arrowhead* in *inset*). The data are consistent with the notion that the end domains contribute to overall filament diameter (Steinert et al., 1983; Eichner et al., 1986; Aebi, et al., 1988). Collectively, our results indicate that a headless and tailless type I keratin K14 can integrate into both simple and epidermal keratin filament networks in vivo, and can assemble into keratin filaments in vitro. These data are also in good agreement with and extend recent studies by Lu and Lane (1990), who showed that a type II keratin K7 mutant, missing all but ~30 residues of the nonhelical amino end and all but ~15 residues of the non-

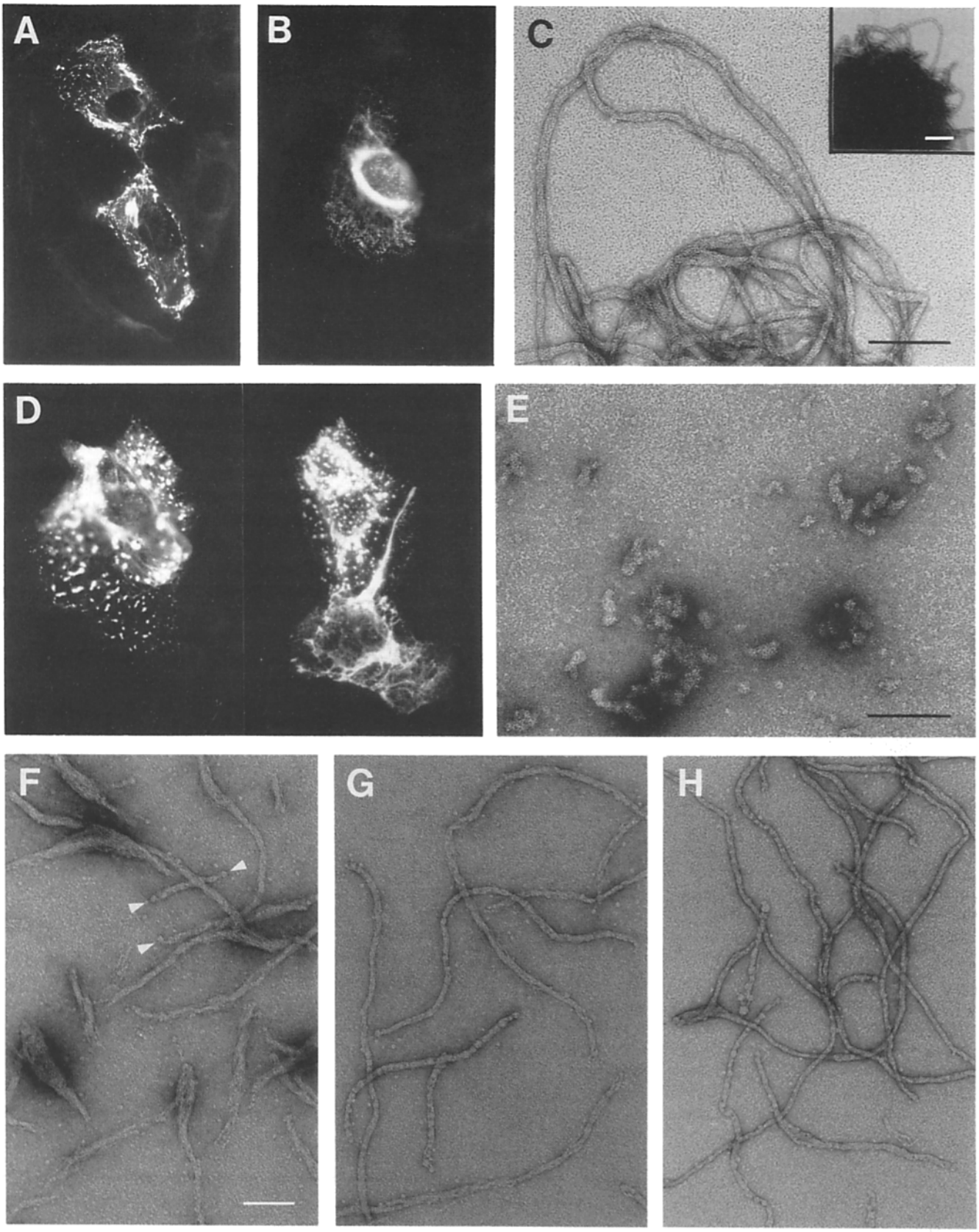

Figure 6. In vivo and in vitro analysis of the carboxy-terminal helical K14 mutants, K14PCΔ73 and K14PCΔ135. PtK2 cells (*A*) or SCC-13 keratinocytes (*B* and *D*) were transfected with pJK14PCΔ73 (*A* and *B*) or pJK14PCΔ135 (*D*) and processed as described in Materials and Methods. K14PCΔ73 and K14PCΔ135 integrated into and colocalized with the endogenous keratin network. Note that collapsed filament networks and punctate staining are present in cells transfected with pJK14PCΔ73, while mainly punctate staining is seen in pJK14PCΔ135-transfected cells. (*C* and *E*) Anion exchange-purified complexes of K5·K14PCΔ73 (*C*) or K5·K14PCΔ135 (*E*) were pro-

helical carboxy tail, assembled a keratin filament network with wild-type keratin K18 (type I) in transfected fibroblasts.

The Amino and Carboxy Nonhelical Sequences Can Influence Interactions Involved in Tetramer Formation

The dramatic sequence diversity in head and tail domains among IF proteins suggested the possibility that these sequences may influence ionic interactions that stabilize the coiled-coil and higher ordered interactions within an IF. This notion was strengthened when we noticed that the rod mutant (K14PNΔ107/CΔ42) required slightly higher salt (135–140 mM Gu·HCl vs. ~110 mM Gu·HCl for K14P) for elution from our anion exchange column, a feature consistent with the differences in predicted pKis of K14P (4.88) vs. K14PNΔ107CΔ42 (4.66). To examine the possibility that K14PNΔ107/CΔ42 may have a greater affinity for K5 than wild-type K14, we combined equimolar amounts of K14PNΔ107/CΔ42 and K14P with half the molar amount of K5 in the presence of 6 M urea and a reducing agent. When tetramers were separated from monomers by anion exchange chromatography, there was a reproducible increase (10–15%) in the amount of mutant in the tetramer peak vs. the starting complex before fractionation (data not shown). This increase could not be accounted for by mere contamination of the tetramer peak by K14PNΔ107/CΔ42 monomers. The data indicate that the rod domain of K14 has a greater affinity for K5 than intact K14, and that tetramer formation is facilitated by removal of the nonhelical sequences. This finding opens the possibility that a part of the variation in the properties of different IFs may arise from differences in ionic interactions imparted by the hypervariable end domains.

K14 Mutants Missing the Highly Conserved R L L E G E Domain at the End of the α-Helical Rod Cause a Collapse of the Filament Network In Vivo, But Assemble into 10-nm Filaments In Vitro

In contrast to the apparent wild-type in vivo behavior of mutants lacking portions of the K14 nonhelical carboxy-terminal domain, the mutant K14PCΔ50, missing only the highly conserved R L L E G E residues at the extreme end of the fourth helical domain, caused a marked collapse of the endogenous keratin filament network in simple epithelial PtK2 cells (Fig. 5). Additional examples of these collapsed networks showing colocalization of endogenous and mutant keratins can be found in Albers and Fuchs (1987). Interestingly, this mutant did not usually have much effect when expressed in cultured keratinocytes, which have a more extensive and stable keratin filament network than do simple epithelial cells. However in a few transfected keratinocytes, K14PCΔ50 showed some evidence of filament network perturbation, including collapse of the endogenous network around the nucleus and small punctate aggregates in the cytoplasm (see example in Fig. 5 *B*).

To begin to understand how this mutant keratin might be eliciting a markedly altered keratin filament network in some, but not all epithelial cells, we examined the ability of K14PCΔ50 to form filaments when combined with K5 in vitro. Fig. 5, *C* and *D* show that remarkably, K14PCΔ50 and K5 assembled into filament-like structures comparable in length and diameter to those formed from intact K14P. This was true even for K14CΔ50, where the P-tag was omitted (not shown). The number of filaments formed was appreciable, a feature best visualized at low magnification (Fig. 5 *C*). Under the conditions used, the efficiency of filament formation was not as great as that seen with intact K14P, as judged by the significant amounts of unassembled or partially assembled subunits in the assembly mixture (see *arrows in Fig. 5 D*). Nevertheless, these data suggested that the filamentous structures seen in transfected cells in vivo were not merely due to the presence of wild-type type I keratins tempering the effects of the mutant, but rather reflected the ability of this mutant to assemble into 10-nm filaments. That the filaments were often collapsed in vivo suggest either that intracellular associations were disrupted or alternatively, that the mutant destabilized the resulting IFs.

Mutants Missing Larger Segments of the α-Helical Rod Domain Show More Severe Mutant Phenotypes In Vivo, and Have Diverse Effects On Keratin Filament Assembly In Vitro

K14PCΔ73, missing 33 amino acid residues at the end of the α-helical rod, showed a more severe perturbation of endogenous PtK2 keratin filament networks than the RLLEGE mutant Fig. 6 *A*). Antibody staining was often punctate, although some filamentous structures were always seen. K14PCΔ73 also produced a greater proportion of nonwild-type IF networks in epidermal cells, where collapsed filament networks and punctate antibody staining were typical (Fig. 6 *B*). As was true for all of our mutant constructs, the frequency of mutant phenotype was always greater in transfected PtK2 cells than in transfected SCC-13 keratinocytes.

When K14PCΔ73 was tested for filament formation in vitro, it assembled into filaments albeit with somewhat wider diameter (~11.5 nm) than normal (Fig. 6 *C*). Most unusually, filaments formed with this mutant had a marked propensity to aggregate, and compacted balls of filaments were prevalent in these mixtures (Fig. 6 *C*, *inset*). This suggested the possibility that some domain of K5 was perhaps unmasked as a consequence of the K14 deletion, and was free to associate in an interfilamentous fashion. The unusual behavior of K14PCΔ73 in vitro suggested that the punctate staining frequently seen in cells transfected with this mutant may not necessarily be an indication of unpolymerized subunits. Collectively, the results obtained with K14PCΔ50 and K14PCΔ73 underscore the inadequacy of utilizing immunofluorescence as a means of assaying whether a mutant IF protein can inhibit filament assembly.

K14PCΔ135, missing almost all of the 2B rod segment, has always generated a more severe mutant phenotype than K14PCΔ50 or K14PCΔ73 (Albers and Fuchs, 1987). When expressed in PtK2 cells, only spheroid bodies were visualized with an anti-P or anti-K8 antiserum (Albers and Fuchs,

cessed for in vitro filament assembly as described in Materials and Methods. Samples were negatively stained and visualized by electron microscopy. (*F–H*). K14PCΔ135 and K14P were combined in either a 1:1 mixture (F), a 1:10 mixture (*G*), or a 1:100 mixture (*H*), followed by mixing with a 20% molar excess of K5 in 6 M urea buffer. Resulting complexes were isolated by chromatography and processed for in vitro assembly and electron microscopy as described in the legend to Fig. 4. Bars, 0.1 μm.

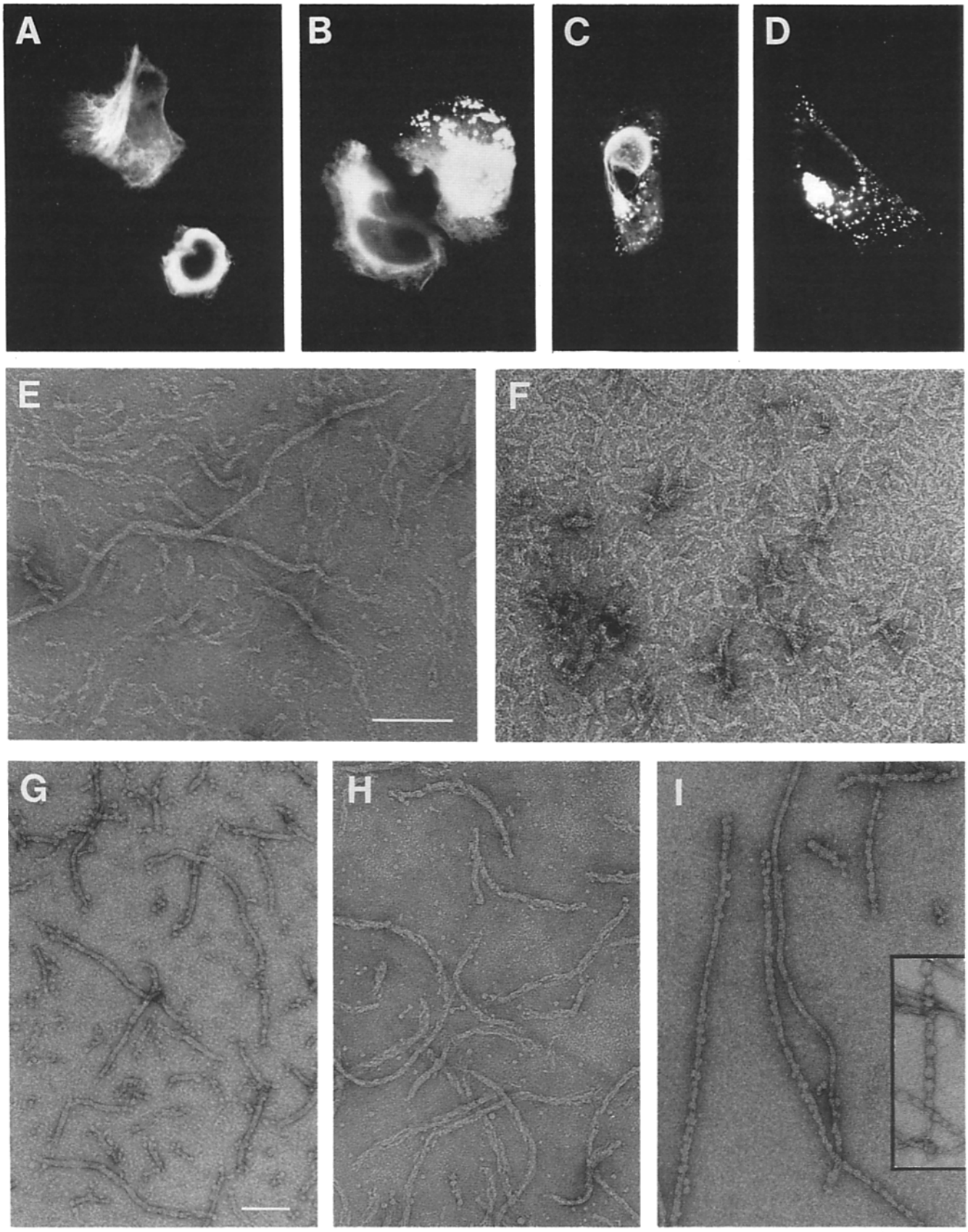

Figure 7. In vivo and in vitro analysis of the amino-terminal helical K14 mutants, K14PNΔ117, K14PNΔ131, and K14PNΔ150. (*A–D*). SCC-13 keratinocytes were transfected with the amino-terminal helical deletion derivatives (pJK14PNΔ117, *A*; pJK14PNΔ131, *B*; pJK14PNΔ150, *C*; and pJK14PNΔ169, *D*), and processed as described in Materials and Methods. These NH_2-terminal mutants usually integrated into and colocalized with most portions of the endogenous keratin network (anti-P, shown; anti-K5, not shown). Note that

1987). Even in transfected keratinocytes, where some wild-type phenotypes were observed, massive disruption of keratin filament networks was sometimes seen, as shown in the examples in Fig. 6 *D*. To determine whether K14PCΔ135 was competent for filament formation in the absence of wild-type K14, we conducted in vitro assembly studies with this mutant and K5. Fig. 6 *E* shows that filament formation was blocked as a consequence of this large K14 deletion. Evidence for elongation was absent, and while interactions between subunits occurred, we could not assess from these data alone whether they were comparable to those that normally take place in the early stages of filament assembly.

The finding that a few pK14PCΔ135-transfected keratinocytes exhibited filamentous structures that were seemingly wild-type prompted us to wonder whether K14PCΔ135 would assemble into 10-nm keratin filaments when combined with intact K14P and K5 in vitro. Fig. 6 *F* indicates that even though elongation was partially restored by addition of equimolar amounts of K14P, filaments were short (635 +/−49 nm) and highly abnormal. Hybrid filaments often showed knob-like projections at their ends (*arrowheads* in Fig. 6 *F*). Interestingly, the filaments were of variable diameter, with a mean of 15.8 +/− 1.0 nm. A few structures were unusually wide, ranging from 30 to 60 nm (these were not included in the calculation of the mean diameter). It is possible that these wide structures represented aggregates of 10-nm fibers. Alternatively, the mechanism that keratins use to calibrate the number of subunits per lateral width may have been perturbed as a consequence of the mutation. Finally, it seemed that interprotofibrillar interactions were somewhat weaker with this COOH-terminal mutant, as judged by the frequent unraveling at filament ends. Whether these weaker interactions contributed to the increased width of the filaments remains unknown.

With increasing amounts of K14P relative to K14PCΔ135 in our assembly mixture, filaments became longer and more nearly 10 nm in diameter (Fig. 6, *G* and *H*). Despite this improvement, filament assembly was still perturbed even when only 1% of the type I keratin was K14PCΔ135 (*H*). Knob-like projections were seen along the length of some filaments and filaments were still shorter than wild-type. The differences observed in filament structures formed with variable amounts of K14P to K14PCΔ135 provide an explanation for the variability observed in our transient transfections of keratinocytes, and furthermore indicate that only a small amount of mutant protein is sufficient to alter filament assembly.

N-Helical K14 Mutants Appear More Severe than C-Helical Mutants in Their Ability to Inhibit Filament Elongation In Vivo and In Vitro

Previously, we showed that an NH_2-terminal K14 mutant K14PNΔ117, missing only a few residues at the extreme end of the first helical domain, caused a marked disruption in the keratin filament network of ~85% of transfected PtK2 cells (Albers and Fuchs, 1989) and ~15% of transfected SCC-13 keratinocytes (Fig. 7 *A*). The phenotype was often, but not always, more perturbed with NH_2-terminal α-helical deletions of greater size (Fig. 7, *B–D*). Phenotypes included (*a*) cytoskeletal keratin networks retracted from the plasma membrane (Fig. 7, *A* and *C*), (*b*) short, wisp-like filamentous fragments and spheroid bodies in the cytoplasm (*B–D*), and (*c*) nuclear aggregates of seemingly nonfilamentous keratin (not shown). The severity of NH_2-terminal mutants seemed to be greater than COOH-terminal mutants, as judged by the greater percentage of transfected SCC-13 keratinocytes showing a mutant phenotype. However, in the absence of knowledge of the ratio of mutant to wild-type K14 in transiently transfected SCC-13 cells, this could not be judged with certainty.

To investigate the effects of NH_2-terminal K14 mutants on filament assembly, we first combined K14PNΔ131 with K5 in vitro. Filament assembly was markedly altered with this mutant (Fig. 7 *E*). Although filament diameter was often close to 10 nm, some variation was evident. In addition, filaments were short, with tapered ends. After the normal 24-h dialysis period, there were still large amounts of partially polymerized subunits, indicative of inefficient assembly. Upon extended assembly periods (up to a week), many of these rodlets associated into longer structures, but the filaments generated were still abnormal. Knob-like projections and side-armed structures were also seen, suggestive of aggregation of the short filament segments with time (not shown).

In contrast to the behavior of K14PNΔ131, K14PNΔ150 nearly quantitatively blocked filament elongation (Fig. 7 *F*). Only short rodlets were observed (mean length, 78 +/− 4 nm), and these usually had tapered ends. Surprisingly, however, the diameter of the rodlets was close to 10 nm, even though the entire 1A α-helical segment was missing. Thus it appeared that K14PNΔ150 was nevertheless capable of coiled-coil and higher ordered lateral interactions. In contrast to the K14PNΔ131 mutant, however, extended assembly periods did not appreciably enhance the efficiency of rodlet formation, nor the length of these structures.

To determine how severe were the effects of K14PNΔ150 on keratin filament formation, we added increasing amounts of K14P relative to K14PNΔ150, and repeated our in vitro reconstitution experiments (Fig. 7, *G–I*). Interestingly, the structures that were obtained with 50% K14P and 50% K14PNΔ150 were quite different from those obtained with 50% K14P and 50% K14PCΔ135 (compare Figure 6 *F* with Fig. 7 *G*). The diameter of the filaments made with the NH_2-terminal mutant was more uniform than that seen with the COOH-terminal mutant. However, filament-forming efficiency and elongation were more severely affected with the NH_2-terminal mutant than with the COOH-terminal one. This was most evident as the filaments were lengthened by adding increasing amounts of K14P to the assembly mixture (Fig. 7, *H* and *I*). Hence when K14PNΔ150 comprised

perinuclear filamentous aggregates were often present. More severe NH_2-terminal mutants generated punctate staining as well. (*E* and *F*) K5·K14PNΔ131 complexes (*E*) and K5·K14PNΔ150 complexes (*F*) were isolated by chromatography and processed for in vitro assembly and electron microscopy as described in the legend to Fig. 4. (*G–I*) K14PNΔ150 and K14P were combined in either a 1:1 mixture (*G*), a 1:10 mixture (*H*), or a 1:100 mixture (*I*), followed by mixing with a 20% excess of K5 in 6 M urea buffer. Anion exchange-purified complexes were processed for in vitro assembly and electron microscopy as described above. Insert in I shows a peculiar beading pattern occasionally seen in the filaments reconstituted in the presence of merely 1% of the K14PNΔ150 mutant. Bars, 0.1 μm. Bar in *E* applies also to *F*. Bar in *G* applies also to *H* and *I*.

Table I. Determination of Width and Length of Filament-like Structures Obtained with K14P Mutant Proteins

Composition of sample*	Width (n = 16)**		Length (n = 40)**	
	Value ‡	C.V.§	Value	C.V.
	nm	%	*nm*	%
K5·K14P (control)	10.5 ± 0.2	6	>2000‖	–
K5·K14PCΔ135	12.4 ± 0.4	16	69 ± 3	31
K5·K14P·K14PCΔ135 50%	15.8 ± 1.0¶	25	635 ± 49	49
K5·K14P·K14PCΔ135 10%	12.5 ± 0.6	20	920 ± 99	67
K5·K14P·K14PCΔ135 1%	10.4 ± 0.3	11	1,166 ± 89	51
K5·K14PNΔ150	10.7 ± 0.6	24	78 ± 4	35
K5·K14P·K14PNΔ150 50%	10.3 ± 0.3	12	224 ± 20	58
K5·K14P·K14PNΔ150 10%	11.6 ± 0.3	10	539 ± 50	59
K5·K14P·K14PNΔ150 1%	10.1 ± 0.3	11	1,049 ± 84	49

* K14P, K14P mutant, or mixture of the two (1, 10, or 50% of mutant) were mixed with a 20% molar excess of K5 in 6 M urea-Tris buffer, and the complex was isolated by anion exchange chromatography as described in Materials and Methods. The pure complex was then processed for in vitro reconstitution of 10-nm filaments. The random sampling procedure performed to obtain these data included only "filament-like" structures (see Materials and Methods for further details).

‡ Values are expressed as means ± SEM.

§ Coefficient of variation, expressed in percentage.

‖ Under the magnification conditions used, K5K14P filaments were too long and convoluted to obtain an unbiased estimate of their length.

¶ In the mixture containing 50% K14PCΔ135, there were both filament-like structures and very short and wide structures. These latter structures were on average 47 ± 2 nm wide (range 30–60 nm; cf. Fig. 6 *F*). These aberrant structures were not used in the compilation of data shown here.

** n = numbers of filaments examined.

only 1% of the total type I keratin in the assembly mix, the efficiency of filament formation was reduced and filaments were slightly shorter than those formed when K14PCΔ135 constituted 1% of the type I keratin. In addition to these differences, a prominent beading pattern along the filament was sometimes seen (Fig. 7 *I*). In some cases, this was highly exaggerated (see *I*, *inset*). The basis for this beading is not known.

To document trends that were readily apparent by qualitative examination of many electron micrographs, we performed quantitative measurements of the mean widths and lengths of randomly selected filament structures formed with varying amounts of K14PCΔ135 and K14PNΔ150 (Table I). While these values must be considered in the context of the limits of resolution afforded by negative staining, they provide the reader with estimations that cannot be gleaned from the small sections of micrographs shown in Fig. 6 and 7. In conclusion, the finding that NH_2-terminal mutants more greatly inhibited filament elongation and filament-forming efficiency than COOH-terminal ones may explain why a greater proportion of aberrant phenotypes were obtained with keratinocytes transfected with NH_2-terminal vs. COOH-terminal mutants.

K14PNΔ150 and K14PCΔ135 Can Still Form Tetramers with Wild-type K5

The fact that K14PNΔ150 and K14PCΔ135 acted in a dominant fashion to disrupt endogenous keratin filament networks in vivo and also interacted with K5 in forming rodlet structures in vitro, was suggestive that these mutants might be able to assemble into heterodimer or heterotetrameric IF precursors. To test this possibility, we conducted anion exchange chromatography on a 6 M urea mixture of (*a*) an excess of K5 and (*b*) either K14P (Fig. 8 *A*), K14PNΔ150 (*B*), or K14PCΔ135 (not shown). Under these conditions, wild-type K5 and K14 exist as heterotetramers (Coulombe and Fuchs, 1990), and eluted as a single species with 130–135 mM guanidinium hydrochloride (Fig. 8 *A*). K14PNΔ150 and K5 also eluted as a single species with 135 mM guanidinium hydrochloride (frame B). When analyzed by SDS PAGE, aliquots of the peak showed a complex of K5 and K14PNΔ150 in a 1:1 molar ratio, as determined by densitometry scanning of the Coomassie blue–stained gel (frame B, gel profile). This 135 mM Gu·HCl peak constituted >95% of the total K14PNΔ150, indicating that similar to intact K14P, most if not all of the mutant K14 was complexed with K5 under these conditions. When this complex was subjected to gel filtration chromatography in the presence of 6 M urea and β-mercaptoethanol, it eluted with an apparent molecular size that was somewhat smaller than the wild-type K5/K14 tetramer but larger than the wild-type heterodimer (Fig. 8 *C*; see small arrow denoting position of myosin standard peak, and see large arrow denoting the relative elution position for the mutant tetramers; see also Coulombe and Fuchs, 1990). The results obtained with the K5/K14PCΔ135 complex were comparable to those obtained with K5/K14PNΔ150. The smaller size of the mutant tetramers is consistent with the smaller sizes of the mutants relative to K14P. Collectively, these data strongly suggest that both the K14PNΔ150 and the K14PCΔ135 mutants can form a coiled-coil interaction with wild-type K5, and in addition, undergo tetramer formation between two mutant coiled-coil dimers with efficiencies indistinguishable from K5·K14P. These findings suggest a basis for the dominant behavior of these mutants in vivo.

Discussion

What Can We Conclude about the Role of Type I Keratin Head and Tail Domains in Filament Assembly In Vitro and in Filament Architecture In Vivo?

While other studies have shown that portions of the rod and/or tail domains are extraneous in keratin filament formation (Steinert et al., 1983; Lu and Lane, 1990), our studies have demonstrated for the first time that a near-perfect headless and tailless keratin, with only a P-tag at the carboxy end of the rod domain, assembled efficiently in vitro with its wild-type type II partner. In part, the apparent dispensability of the type I keratin head and tail domains in our in vivo and in vitro studies is likely to arise from the fact that keratins are obligate heteropolymers. Thus, the head and tail domain of K5 may be sufficient for the K14·K5 heterodimer to assemble into higher ordered structures, a notion which is supported by recent studies of Lu and Lane (1990). While the requirement for heteropolymerization may lessen the importance of keratin ends, it is becoming increasingly clear that other factors also contribute to determining whether a particular end domain will be essential for IF formation. Hence, for example, even when a headless mutant of the neurofilament 68-kD subunit composed only 10% of the total IF protein in transfected fibroblasts, it integrated into, and caused disruption of the resulting vimentin network (Gill et al.,

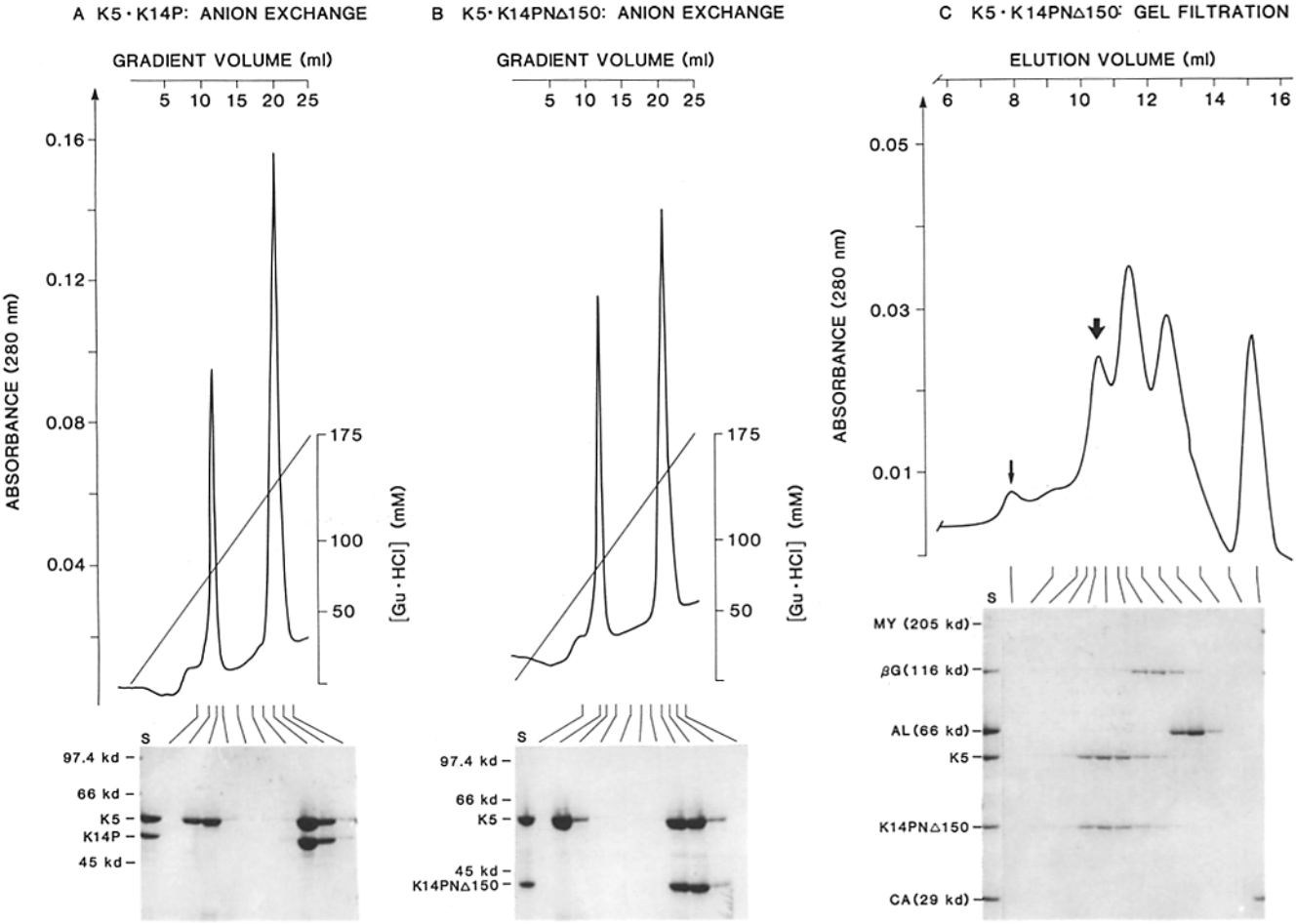

Figure 8. Anion exchange and gel filtration analysis of heterotetrameric complexes formed upon combining K5 and either K14P or K14PNΔ150 in 6 M urea. (*A* and *B*) Anion-exchange chromatography. Purified K5 and either K14P or K14PNΔ150 were combined in a 1.25:1 molar ratio, each at 1 mg/ml in 6 M urea buffer. Complexes were isolated by anion-exchange chromatography and aliquots (30 μl) of each fraction were analyzed by electrophoresis through SDS polyacrylamide gels, followed by staining with Coomassie blue (shown below each UV absorbance profile in the diagram). From left to right, first lane (*S*) represents a 6-μl aliquot of protein used in the analysis and vertical bars over protein profiles indicate sequential fractions examined by SDS-PAGE. Keratin combinations were: *A*, K5 and K14P; *B*, K5 and K14PNΔ150. Sizes of molecular mass standards are indicated at left in kilodaltons. (*C*) Gel filtration. The K5-K14PNΔ150 complex purified by anion-exchange chromatography was combined with molecular mass standards and subjected to gel filtration chromatography in 6 M urea (Coulombe and Fuchs, 1990). Fractions (0.1 ml) were collected and analyzed by electrophoresis through SDS polyacrylamide gels, followed by staining with Coomassie blue (shown below the UV absorbance profile in the diagram). From left to right, first lane (*S*) represents an aliquot (6 μl) of protein used in the analysis, and vertical bars over protein profiles indicate sequential fractions examined by SDS-PAGE. Sizes of molecular mass standards are indicated at left. Thin arrow denotes the myosin peak, which was barely visible by Coomassie blue staining. Thick arrow denotes the K5-K14PNΔ150 complex. Comparison of the mobility of the K5-K14PNΔ150 complex with that of K5-K14P tetramers (not shown; see Coulombe and Fuchs, 1990), indicate that the K5-K14PNΔ150 complexes are stable heterotetramers. Note that the mobility of the heterotetramer in 6 M urea is aberrant, relative to the random-coil molecular mass standards, as noted previously (see Coulombe and Fuchs, 1990, for discussion).

1990). Moreover, in elegant point mutagenesis studies on the nuclear lamins, it was shown by McKeon and co-workers (Heald and McKeon, 1990) that specific serine sequences in the nonhelical amino-terminal domain were essential for the phosphorylation-mediated control of the nuclear lamina assembly. The relative amount of lamin mutant necessary to elicit this response was not determined, nor was it known whether this region is essential for nuclear lamin filament formation per se. However, it seems reasonable that for other IF proteins, especially those that show phosphorylation-mediated alterations in their networks during mitosis, the end domains may be more important than they are for the epidermal keratin filaments, which appear to remain intact throughout the cell cycle. Interestingly, in this regard, the highly conserved serine residues that are essential for nuclear lamina formation and are substrates for the cdc2 kinase (Ward and Kirschner, 1990; Heald and McKeon, 1990; Peter et al., 1990) are not present at the corresponding positions of the K14 nonhelical domains.

Our data do not necessarily imply that the nonhelical domains of K14 are entirely dispensable in vivo as they seem to be in vitro. In this regard, it must be recognized that our

in vivo studies were limited to expression of type I mutants in cells that express an endogenous keratin filament network. Here, we are faced with a dilemma, because to express mutant type I and type II keratins in cells that do not have keratin networks and keratin-associated structures (e.g., desmosomes) is an artificial situation in itself, and hence may not be meaningful from a functional standpoint (Giudice and Fuchs, 1987; Lu and Lane, 1990). On the other hand, our tailless/headless mutants may have no apparent effect on transfected epithelial cells only because the wild-type type I K14 compensates for the mutant. To properly answer whether in conjunction with K5, our K14 rod mutant can form a wild-type keratin filament network replete with desmosomal contacts and other IF associations, we would need to conduct homologous recombination studies to replace K14 wild-type expression with K14 mutant expression. Alternative cell biological approaches (Georgatos and Blobel, 1987*a*,*b*) may also provide valuable information regarding the role of the end domains in filament network interactions with other cellular organelles/structures in vivo.

What Can We Conclude about the Role of the α-Helical Domains in Filament Assembly and Architecture?

We knew from our prior in vivo studies that deletions into the α-helical domains of K14 resulted in mutants unable to form a proper keratin filament network in epithelial cells in culture (Albers and Fuchs, 1987; 1989). From these studies alone, however, we could not discern whether the mutants caused (*a*) an inherent disruption in the assembly process per se, (*b*) alterations in the interactions between IFs and other cellular structures (e.g., desmosomes), or (*c*) alterations in IF stability and/or interfilament interactions. Our in vitro studies enabled us to distinguish between the fundamental issue of whether our mutant subunits were competent to assemble into 10-nm filaments. While our studies did not unequivocally distinguish between (*b*) and (*c*), they often provided a clue as to the extent to which (*c*) may have contributed to the in vivo phenotype.

We were surprised to discover that deletion of the most highly conserved L L E G E sequence at the COOH-terminal end of the α-helical rod domain had only minor effects on the ability of mutant K14PCΔ50 or K14CΔ50 subunits to assemble in vitro into 10-nm filaments. While keratinocytes transfected with these mutants usually showed a wild-type phenotype, it was always suspected that this was due to the presence of endogenous wild-type K14 tempering the effects of the mutant. Even more astonishing was the finding that the K14PCΔ73 mutant, missing an additional 23 rod residues, assembled in vitro into 11–12-nm filaments. K14PCΔ73-transfected cells often showed punctate staining of the keratin network, and it had seemed likely that this was due to disruption in filament assembly (Albers and Fuchs, 1987). It now seems more likely that the punctate staining arose from filament aggregates. We do not yet know whether the rod domain has functions in addition to those involved in filament formation, and hence our correlations between the in vitro and in vivo behavior of the mutants cannot be made with certainty. However, the surprising feature of these comparisons is that they seem to correlate very well, suggesting that the effects of endogenous type I keratins on the in vivo phenotypes may have been minimal.

In contrast to the more subtle effects of K14PCΔ50 and K14PCΔ73 mutants on in vitro keratin filament assembly, more extensive deletions at the carboxy or amino ends of the α-helical domain resulted in major distortions of the assembly process. Overall, both amino and carboxy K14 deletion mutants formed complexes with K5 that associated laterally better than end-to-end. This was confirmed by our chromatographic studies, which showed that even mutants with large α-helical deletions formed remarkably stable tetramers, and yet were not able to form fibers with appreciable length. In addition, our studies revealed a marked difference between the behavior of the severe carboxy α-helical mutants and of the amino α-helical mutants. While the carboxy mutants generated abnormalities either in calibrating filament diameter or in lateral aggregation, amino mutants generated structures that were often close to 10 nm in diameter. In contrast, deletions at the amino end of the rod domain affected elongation more severely than deletions at the carboxy end. Interestingly, for both carboxy and amino helical deletions, concentrations of 1% were sufficient to perturb filament formation. However, even at these low mutant concentrations, elongation was still more affected with the amino helical mutants than with the carboxy ones.

How Do Our Findings with Type I Keratin Mutants Relate to In Vivo and In Vitro Assembly Studies with Other IF Proteins?

Because of the obligate heteropolymer requirements for keratins and because of their extraordinary stability, we believe that our in vitro studies on epidermal keratin filament formation have defined sequences that will be required, but not sufficient, for the assembly of all IFs. In this regard, our studies clearly point to the rod domain as being an essential component of the assembly process. In addition, the differences between our K14PNΔ107 and K14PNΔ115 mutants in keratin filament assembly have indicated a more precise demarcation in the amino boundary of the rod, and given the high degree of evolutionary conservation within this region, it seems likely that this demarcation will be similar for most if not all IFs. Similarly, the differences between K14PCΔ42 and K14PCΔ50 mutants in efficiency of keratin filament assembly suggest a demarcation of the carboxy end of the rod that is likely to apply for most other IF polypeptides. The fact that K5K14PCΔ50 filaments were longer and formed with greater efficiency than K5K14PNΔ115 filaments suggests that the NH_2-terminal end of the rod domain may play a more crucial role in filament formation than the COOH-terminal end, a finding that was not predicted on the basis of sequence comparisons alone, but a finding which we expect will apply to all IFs.

In contrast to our studies on the α-helical domains of K14, our truncation studies on the nonhelical domains may apply only to keratins, and similar studies by Lu and Lane (1990) suggest that simple epithelial keratins as well as epidermal keratins may be able to form 10-nm filaments even when one of the keratin pair is headless and tailless. Previously, it was suggested that the inability of our K14 rod to generate a mutant phenotype in vivo was probably due to its low concentration relative to wild-type keratins (Raats et al., 1990). Our in vitro studies now make it more likely that there are fundamental differences between the behavior of truncated forms of desmin (Raats et al., 1990), NF-L (Gill et al.,

1990), NF-M (Wong and Cleveland, 1990), and K14 (Albers and Fuchs, 1987, 1989) in vivo, and quite possibly in vitro as well. While it would be surprising if keratin filaments could assemble from two keratin rod mutants, the in vivo and in vitro differences between keratins and other IF proteins seem to go beyond the mere difference in homopolymer versus heteropolymer formation.

As more truncated and point mutant IF proteins are analyzed both for their ability to form IF networks in vivo and for their ability to form 10-nm filaments in vitro, a clearer picture should emerge as to the extent to which (*a*) sequences necessary for IF assembly will differ from those necessary for IF network formation, and (*b*) sequences necessary for either of these events will vary among IF classes or even among individual proteins within an IF class.

We would like to extend a very special thank you to Dr. Robert Josephs and Gerald Grofman for their most generous help and advice concerning techniques of electron microscopy, use of their electron microscope, and expert developing of the micrographs presented in this manuscript. We also thank Ms. Grazina Traska for her valuable assistance in tissue culture. Finally, we thank Philip Galiga for his artful presentation of the data.

This work is supported by a grant from the National Institutes of Health (AR27883). E. Fuchs is an Investigator of the Howard Hughes Medical Institute. P. A. Coulombe is the recipient of a Centennial Fellowship from the Medical Research Council of Canada.

Received for publication 28 August 1990 and in revised form 19 September 1990.

References

Aebi, U., J. Cohn, L. Buhle, and L. Gerace. 1986. The nuclear lamina is a meshwork of intermediate-type filaments. *Nature (Lond.).* 323:560–564.

Aebi, U., M. Haner, J. Troncoso, R. Eichner, and A. Engel. 1988. Unifying principles in intermediate filament (IF) structure and assembly. *Protoplasma (Berl.).* 145:73–81.

Ahmadi, B., and P. T. Speakman. 1978. Suberimidate crosslinking shows that a rod-shaped low-cysteine high-helix protein prepared by limited proteolysis of reduced wool has four protein chains. *FEBS (Fed. Eur. Biochem. Soc.) Lett.* 94:365–367.

Albers, K., and E. Fuchs. 1987. The expression of mutant epidermal keratin cDNAs transfected in simple epithelial and squamous cell carcinoma lines. *J. Cell Biol.* 105:791–806.

Albers, K., and E. Fuchs. 1989. Expression of mutant keratin cDNAs in epithelial cells reveals possible mechanisms for initiation and assembly of intermediate filaments. *J. Cell Biol.* 108:1477–1493.

Bader, B. L., T. M. Magin, M. Hatzfeld, and W. W. Franke. 1986. Amino acid sequence and gene organization of cytokeratin no. 19, an exceptional tail-less intermediate filament protein. *EMBO (Eur. Mol. Biol. Organ.) J.* 5:1865–1875.

Bradford, M. M. 1976. A rapid and sensitive method for the quantitation of microgram quantities of protein utilizing the principle of protein-dye binding. *Anal. Biochem.* 72:259–254.

Chou, P. Y., and G., D. Fasman. 1978. Prediction of the secondary structure of proteins from their amino acid sequence. *Adv. Enzymol.* 47:45–148.

Chou, Y. H., E. Rosevear. and R. D. Goldman. 1989. Phosphorylation and disassembly of intermediate filaments in mitotic cells. *Proc. Natl. Acad. Sci. USA.* 86:1885–1889.

Coulombe, P., and E. Fuchs. 1990. Elucidating the early stages of keratin filament assembly. *J. Cell Biol.* 111:153–169.

Engel, A., R. Eichner, and U. Aebi. 1985. Polymorphism of reconstituted human epidermal keratin filaments: determination of their mass-per-length and width by scanning transmission electron microscopy (STEM). *J. Ultrastruc. Res.* 90:323–335.

Evans, R. M. 1988. The intermediate-filament proteins vimentin and desmin are phosphorylation in specific domains. *Eur. J. Cell Biol.* 46:152–160.

Evans, R. M. 1989. Phosphorylation of vimentin in mitotically selected cells. In vitro cyclic AMP-independent kinase and calcium-stimulated phosphatase activities. *J. Cell Biol.* 108:67–78.

Fisher, D. Z., N. Chaudhary, and G. Blobel. 1986. CDNA sequencing of nuclear lamins A and C reveals primary and secondary structural homology to intermediate filament proteins. *Proc. Natl. Acad. Sci. USA.* 83:6450–6454.

Franke, W. W., D. L. Schiller, M. Hatzfeld, and S. Winter. 1983. Protein complexes of intermediate-sized filaments: melting of cytokeratin complexes in urea reveals different polypeptide separation characteristics. *Proc. Natl. Acad. Sci. USA.* 80:7113–7117.

Geisler, N., and K. Weber. 1982. The amino acid sequence of chicken muscle desmin provides a common structural model for intermediate filament proteins. *EMBO (Eur. Mol. Biol. Organ.) J.* 1:1649–1656.

Geisler, N., and K. Weber. 1988. Phosphorylation of desmin in vitro inhibits formation of intermediate filaments; identification of three kinase A sites in the amino terminal head domain. *EMBO (Eur. Mol. Biol. Organ.) J.* 7:15–20.

Geisler, N., M. Hatzfeld, and K. Weber. 1989. Phosphorylation in vitro of vimentin by protein kinase A and C is restricted to the head domain. *Eur. J. Biochem.* 183:441–447.

Georgatos, S. D., and G. Blobel. 1987*a*. Two distinct attachment sites for vimentin along the plasma membrane and the nuclear envelope in avian erythrocytes: a basis for a vectorial assembly of intermediate filaments. *J. Cell Biol.* 105:105–115.

Georgatos, S. D., and G. Blobel. 1987*b*. Lamin B constitutes an intermediate filament attachment site at the nuclear envelope. *J. Cell Biol.* 105:117–125.

Georgatos, S. D., D. C. Weaver, and V. T. Marchesi. 1985. Site specificity in vimentin-membrane interactions: intermediate filament subunits associate with the plasma membrane via their head domains. *J. Cell Biol.* 101:1962–1967.

Gill, S. R., P. C. Wong, and D. W. Cleveland. 1990. Assembly properties of dominant and recessive mutations in the small mouse neurofilament (NF-L) subunit. *J. Cell Biol.* 111:2005–2020.

Giudice, G. J., and E. Fuchs. 1987. The transfection of human epidermal keratin genes into fibroblasts and simple epithelial cells: evidence for inducing a type I keratin by a type II gene. *Cell.* 48:453–463.

Hanukoglu, I., and E. Fuchs. 1982. The cDNA sequence of a human epidermal keratin: divergence of sequence but conservation of structure among intermediate filament proteins. *Cell.* 31:243–252.

Hatzfeld, M., and W. W. Franke. 1985. Pair formation and promiscuity of cytokeratins: formation in vitro of heterotypic complexes and intermediate-sized filaments by homologous and heterologous recombinations of purified polypeptides. *J. Cell Biol.* 101:1826–1841.

Hatzfeld, M., and K. Weber. 1990. The coiled coil of in vitro assembled keratin filaments is a heterodimer of type I and II keratins: use of site-specific mutagenesis and recombinant protein expression. *J. Cell Biol.* 110:1199–1210.

Heald, R., and F. McKeon. 1990. Mutations of phosphorylation sites in lamin A that prevent nuclear lamina disassembly in mitosis. *Cell.* 61:579–589.

Henderson, D., N. Geisler, and K. Weber. 1982. A periodic ultrastructure in intermediate filaments. *J. Mol. Biol.* 155:173–176.

Inagaki, M., Y. Nishi, K. Nishizawa, M. Matsuyama, and C. Sato. 1987. Site-specific phosphorylation induces disassembly of vimentin filaments. *Nature (Lond.).* 328:649–652.

Kaufman, E., K. Weber, and N. Geisler. 1985. Intermediate filament forming ability of desmin derivatives lacking either the amino-terminal 67 or the carboxy-terminal 27 residues. *J. Mol. Biol.* 185:733–742.

Kitamura, S., S. Ando, M. Shibata, K. Tanabe, C. Sato, and M. Inagaki. 1989. Protein kinase-C phosphorylation of desmin at four serine residues within the non-alpha-helical head domain. *J. Biol. Chem.* 264:5674–5678.

Lane, E. B. 1982. Monoclonal antibodies provide specific intramolecular markers for the study of epithelial tonofilament organization. *J. Cell Biol.* 92:665–673.

Loewinger, L., and F. McKeon. 1988. Mutations in the nuclear lamin proteins resulting in their aberrant assembly in the cytoplasm. *EMBO (Eur. Mol. Biol. Organ.) J.* 7:2301–2309.

Lu, X., and B. Lane. 1990. Use of retrovirus vectors to express defective keratins in non-epithelial cells: two types of binding sites involved in keratin polymerization. *Cell.* 62:681–696.

Marchuk, D., S. McCrohon, and E. Fuchs. 1984. Remarkable conservation of structure among intermediate filament genes. *Cell.* 39:491–498.

McKeon, F. M., M. W. Kirschner, and D. Caputo. 1986. Homologies in both primary and secondary structure between nuclear envelope and intermediate filament proteins. *Nature (Lond.).* 319:463–468.

McLachlan, A. D. 1978. Coiled-coil formation and sequence regularities in the helical regions of α-keratins. *J. Mol. Biol.* 124:297–304.

McLachlan, A. D., and M. Stewart. 1982. Periodic charge distribution in the intermediate filament proteins desmin and vimentin. *J. Mol. Biol.* 162: 693–698.

Parry, D. A. D., W. G. Crewther, R. D. Fraser, and T. P. MacRae. 1977. Structure of α-keratin: structural implications of the amino acid sequence of the type I and type II chain segments. *J. Mol. Biol.* 113:449–454.

Peter, M., J. Nakagawa, M. Doree, J. C. Labbe, and E. A. Nigg. 1990. In vitro disassembly of the nuclear lamina and M phase-specific phosphorylation of lamins by cdc2 kinase. *Cell.* 61:591–602.

Quinlan, R. A., and W. W. Franke. 1982. Heteropolymer filaments of vimentin and desmin in vascular smooth muscle tissue and cultured baby hamster kidney cells demonstrated by chemical crosslinking. *Proc. Natl. Acad. Sci. USA.* 79:3452–3456.

Quinlan, R. A., J. A. Cohlberg, D. L. Schiller, M. Hatzfeld, and W. W. Franke. 1984. Heterotypic tetramer (A2D2) complexes of non-epidermal keratins isolated from cytoskeletons of rat hepatocytes and hepatoma cells. *J. Mol. Biol.* 178:365–388.

Raats, J. M. H., F. R. Pieper, Egberts Vree, T. M. Wilma, K. N. Verrijp, Frans C. S. Ramaekers, and H. Bloemendal. 1990. Assembly of amino terminally deleted desmin in vimentin-free cells. *J. Cell Biol.* 111:1971–1986.

Sauk, J. J., M. Krumweide, D. Cocking-Johnson, and J. G. White. 1984. Reconstitution of cytokeratin filaments in vitro: Further evidence for the role of nonhelical peptides in filament assembly. *J. Cell Biol.* 99:1590–1597.

Steinert, P. M. 1988. The dynamic phosphorylation of the human intermediate filament keratin 1 chain. *J. Biol. Chem.* 263:13333–13339.

Steinert, P. M. 1990. The two-chain coiled-coil molecular of native epidermal keratin intermediate filaments is a type I-type II heterodimer. *J Biol. Chem.* 265:8766–8774.

Steinert, P. M., W. W. Idler, and S. B. Zimmermann. 1976. Self assembly of bovine epidermal keratin filaments in vitro. *J. Mol. Biol.* 108:547–567.

Steinert, P. M., R. H. Rice, D. R. R., and B. L. Trus, A. C. S. 1983. Complete amino acid sequence of a mouse epidermal keratin subunit and implications for the structure of intermediate filaments. *Nature (Lond.).* 302:794–800.

Steven, A., J. Hainfeld, B. Trus, J. Wall, and P. Steinert. 1983. Epidermal keratin filaments assembled in vitro have masses-per-unit length that scale according to average subunit masses: structural basis for homologous packing of subunits in intermediate filaments. *J. Cell Biol.* 97:1939–1944.

Sun, T.-T., R. Eichner, A. Schermer, D. Cooper, W. G. Nelson, and R. A. Weiss. 1984. The Transformed Phenotype. *In* Cancer Cells, Vol. 1. A. Levine, W. Topp, G. van de Woude, and J. D. Watson, editors. Cold Spring Harbor Laboratory, Cold Spring Harbor, New York. 169–176.

Van den Heuvel, R. M. M., G. J. M. M., van Eys, F. C. S. Ramaekers, W. J. Quax, W. T. M. Vree-Egberts, G. Schaart, H. T. M. Cuypers, and H. Bloemendal. 1987. Intermediate filament formation after transfection with modified hamster vimentin and desmin genes. *J. Cell Sci.* 88:475–482.

Ward, G. E., and M. W. Kirschner. 1990. Identification of cell cycle-regulated phosphorylation sites on nuclear lamin C. *Cell.* 61:561–577.

Weber, K., and N. Geisler. 1987. Biochemistry and molecular structure of intermediate filaments. *In* Nature and Function of Cytoskeletal Proteins in Motility and Transport. G. Fischer, editor. Stuttgart Verlag, Federal Republic of Germany. 251–260.

Wong, P. C., and D. W. Cleveland, 1990. Characterization of dominant and recessive assembly defective mutations in mouse neurofilament NF-M. *J. Cell Biol.* 111:1987–2004.

Woods, E. F., and A. S. Inglis. 1984. Organization of the coiled-coils in the wool microfibril. *Int. J. Biol. Macromol.* 6:277–283.